Supplementary Information for: Room temperature experimental implementation of quantum logic on a hybrid magnon-spin system

1. IMAGING OF NV CENTERS IN DIAMOND

To maximize signal contrast, we utilize a home-built confocal microscope with a laser power of 0.5 mW to analyze the fluorescence wavelengths of NV centers (SFig. 1a) and the stray light from YIG films (SFig. 1b). In SFig. 1c, it is observed that the maximum signal-to-noise ratio (approximately 5) for single NV center imaging is achieved when collecting fluorescence in the wavelength range between 650 nm and 700 nm. The spacing between each pair of NV center points is 2 μm, determined from the mask pattern. The point indicated by the black circle represents a single NV center, with approximately 30 k/s for its fluorescence counts and 6 k/s for background noise counts.

Subsequently, we characterize the second-order correlation function of this NV center, resulting in $g^2(0) = 0.29$ which is below 0.5, confirming its single NV center nature. Furthermore, we employe microwave (MW) driving to assess its coherent properties at a resonance frequency of approximately 2.1 GHz (similar to the main text in Fig. 2e). As depicted in SFig. 1e and SFig. 1f, the Ramsey signal is fitted using the equation $Ae^{-(t/T_2^*)^2}\cos(2\pi\Delta t + \phi) + B$, where Δ is 2.14 MHz due to coupling with the ^{14}N nuclear spin, and T_2^* is 1.32(8) μs, The spin echo envelope is fitted by $Ae^{-t/T_2} + B$, with T_2 equal to 40(1) μs, similar to the results for magnon driving in the main text.

2. MEASUREMENT OF MAGNETOSTATIC SURFACE SPIN WAVE WAVELENGTH

The short wavelength characteristic of magnetostatic surface spin waves (MSSW) is a prominent advantage for locally manipulating other quantum qubits using magnons. As shown in SFig. 2, the NV center in diamond near the microstrip line (~ 10 μm) can be driven by both magnons and MW fields. Their interference produces periodic modulation in the photoluminescence excitation (PL) intensity and Rabi frequency of the NV center. As a result, the Rabi frequency of the NV center can be expressed as follows:

$$\Omega_{Rabi}(y) = \sqrt{2}\gamma \left| B_{SW} \cos^2\left(\frac{\phi}{2}\right) e^{ik_y y} - B_{MW}(y) \right|$$

where B_{SW} represents amplitude of MSSW, it can be treated as approximately constant within the range of several micrometers for YIG films, $\phi = 35°$ is the angle between the NV center axis and the YIG film plane, which is determined by the axial direction of [100]-oriented diamond. The $\gamma/2\pi = 28$ MHz/mT is the electron gyromagnetic ratio, k_y is wave vector of propagation direction, $B_{MW}(y)$ is the magnetic field generated by MW. We obtain the wavelength of MSSW ranging from 2.1 GHz to 2.5 GHz through periodic changes in the Rabi frequency. The measurable MSSW wavelength falls between 3 μm and 15 μm.

3. CHARACTERIZATION OF MW CURRENT HEATING EFFECT

To confirm the existence of MW current heating effects, we initially investigate the resonance frequency shift of the NV center in three cases: before MW heating, after 1 minute of MW heating, and after 1 hour without MW heating. The power of the MW currents is set at 33 dBm, and the frequency is 1 GHz and detune with the NV center. We observe a frequency shift of approximately 650 kHz after MW heating. As the NV center's resonance frequency shifts due to Joule heating from the MW current and detunes with magnons driving, the amplitude of the Rabi oscillation signal of the NV center decreases, and the effective Rabi frequency increases, as shown in SFig. 3.

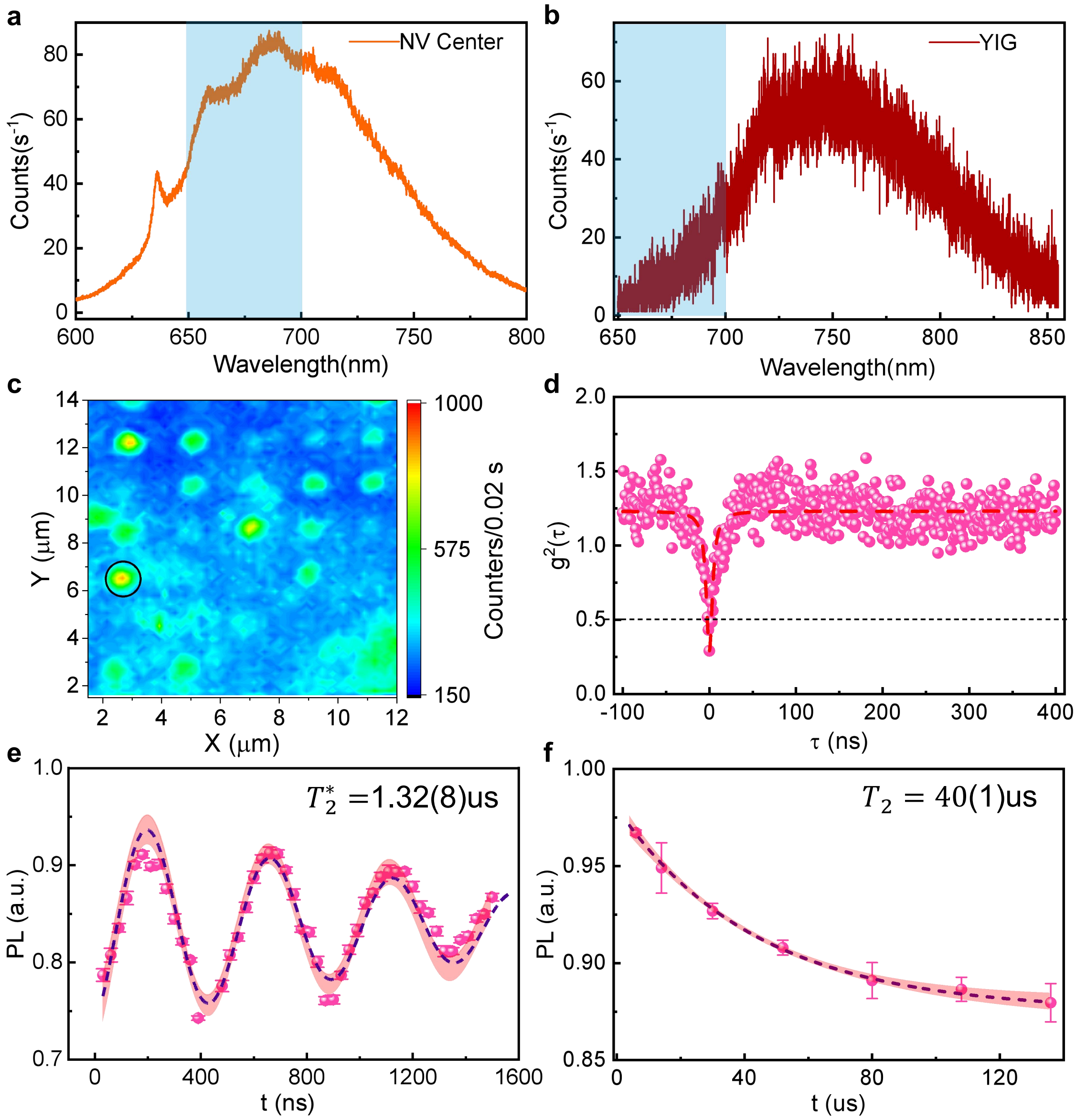

SFig. 1: **The photoluminescence excitation (PLE) spectra of our hybrid quantum system at room temperature.** **a** PLE spectra of NV center in diamond. **b** Stray light spectrum of YIG films. To achieve high signal-to-noise ratio for single NV center imaging and identification, we collecte the NV center's fluorescence of wavelength range between 650 nm and 700 nm (denotes with gray region) with two optical filters. **c** Confocal image of the NV centers used in the experiment. **d** Second-order intensity-correlation measurement for the single NV center at 0.5 mW, the red dash line is a theoretical fit. **e** Ramsey oscillations of single NV center with MW driving. **f** Spin echo signal of single NV center with MW driving.

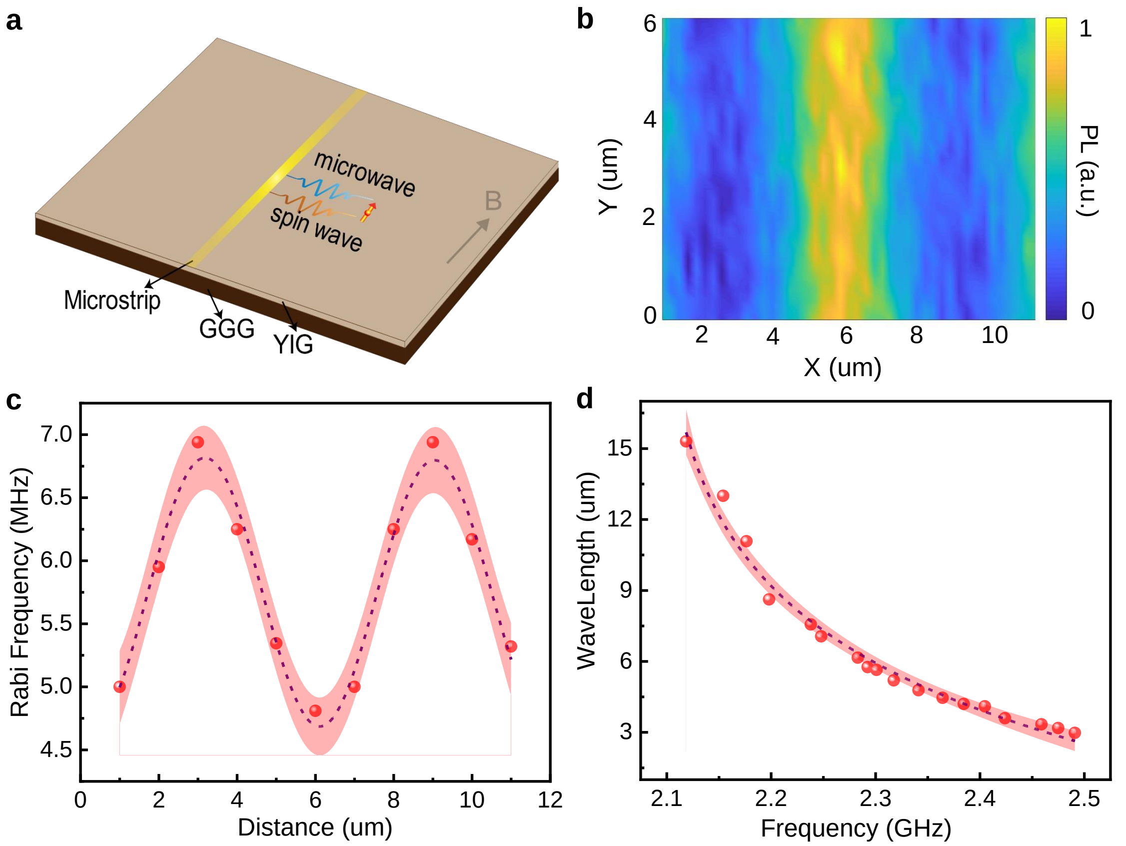

SFig. 2: **The relationship between frequency and wavelength of MSSW.** **a** Illustration of measurement for MSSW wavelength of YIG film. **b** Imaging of NV center's normalized PL on the right side of microstrip line with driving frequency 2.283 GHz. **c** Periodic modulation of Rabi frequency of NV center on magnons propagation direction. **d** The variation of wavelength with driving frequency.

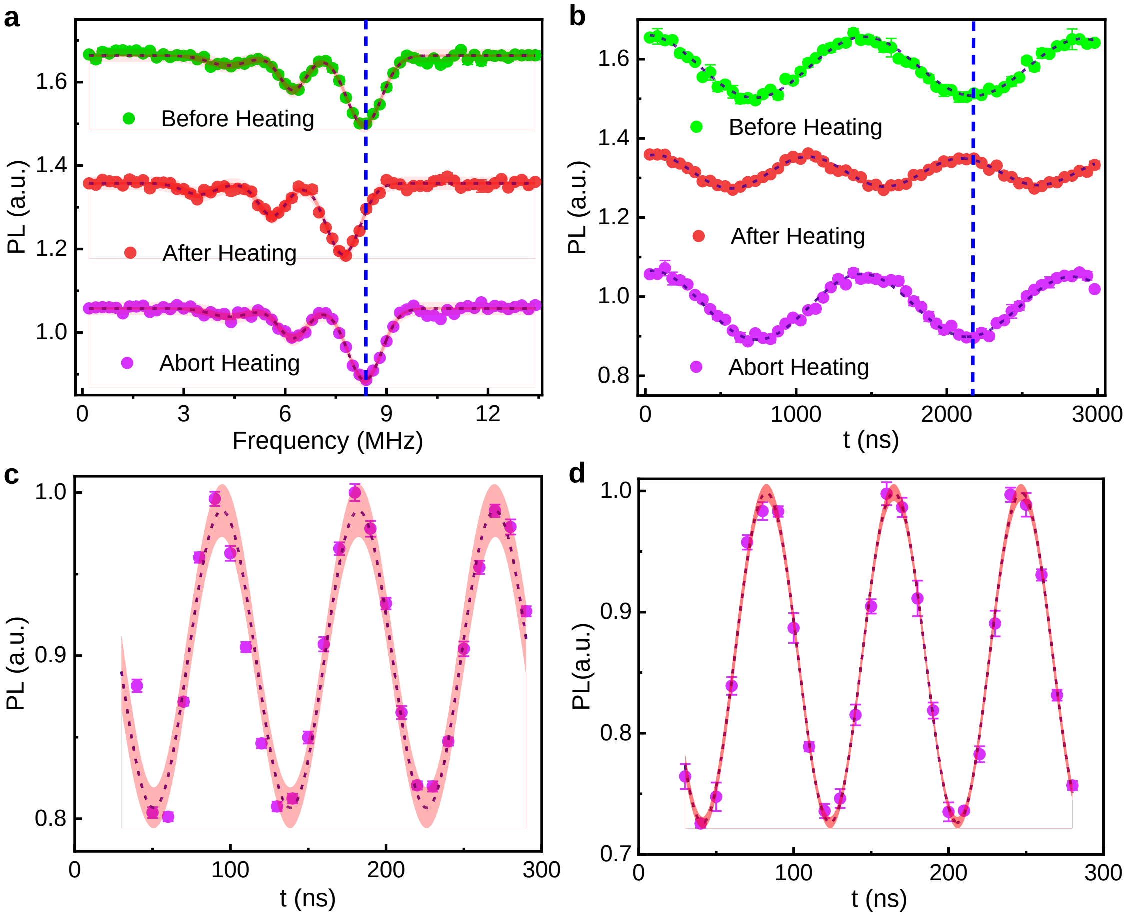

SFig. 3: **The Joule heating effect of MW current.** **a** The electron spin resonance (ESR) frequency of NV center measurements with magnons driving for before MW heating, after MW heating, and abort MW heating (1 GHz, 33 dBm) separately. **b** Maintaining the magnons driving frequency and power of MW currents in picture **a** and measuring Rabi oscillation signal in three different conditions. **c** Rabi oscillation of NV center with MW driving. **d** Rabi oscillation of NV center with magnons driving. (Similar Rabi oscillation frequencies correspond to the Fig. 3c in the main text, are 12.1 MHz and 11.4 MHz respectively.)

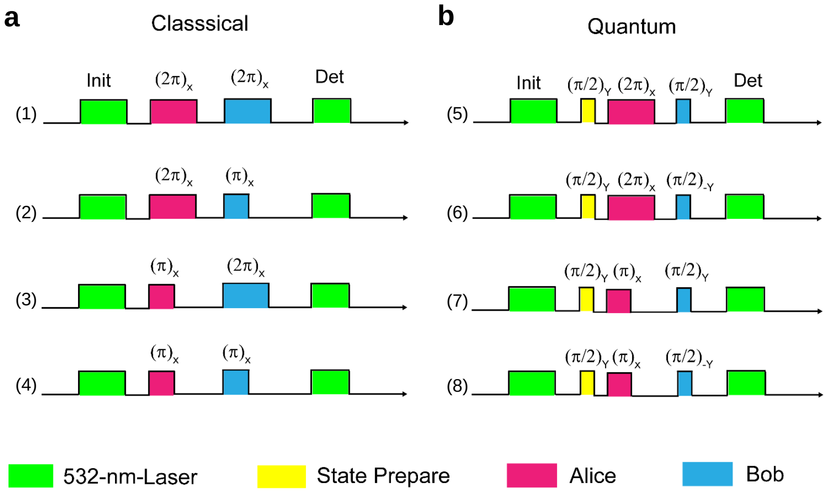

SFig. 4: **Experiment sequences for quantum game for main text Figure 4.** **a** Classical scenario. The operation sequences 1 to 4 are corresponding to strategy of $(S_A = I, S_B = I)$, $(S_A = I, S_B = X)$, $(S_A = X, S_B = I)$, $(S_A = X, S_B = X)$. **b** Quantum scenario. The operation sequences 5 to 8 are corresponding to strategy of $(S_A = I, S_B = Y/2)$, $(S_A = I, S_B = -Y/2)$, $(S_A = X, S_B = Y/2)$, $(S_A = X, S_B = -Y/2)$.